Structures and Phase Transitions of α-Bis(*N*-methylsalicylaldiminato)nickel(II)*

By W. Steurer and W. Adlhart

Institut für Kristallographie und Mineralogie der Universität München, Theresienstrasse 41, 8000 *München* 2,
Federal Republic of Germany

Abstract

The title compound (α-NiNSal) shows a continuous phase transition from an orthorhombic $[T > 205\,(3)\,\text{K}]$ to an incommensurate modulated phase with orthorhombic average structure. The one-dimensional displacively modulated structure is transformed by a first-order phase transition into a monoclinic modification $[T < 153\,(2)\,\text{K}]$. The crystal structures at room temperature (A), at 160 K (B) and 40 K (C) have been determined by single-crystal X-ray methods. (A): $Iba2$, $Z = 4$, $a = 9\cdot167\,(2)$, $b = 24\cdot282\,(4)$, $c = 6\cdot597\,(1)$ Å, $U = 1469\,\text{Å}^3$, $D_x = 1\cdot48$ g cm^{-3}, $R = 0\cdot067$, $R_w = 0\cdot032$ for 1238 unique reflexions. (B): Average structure: $Iba2$, $Z = 4$, $a = 9\cdot09\,(3)$, $b = 24\cdot13\,(7)$, $c = 6\cdot43\,(2)$ Å, $U = 1410\,\text{Å}^3$, $D_x = 1\cdot54$ g cm^{-3}, $R = 0\cdot065$, $R_w = 0\cdot026$ for 1480 unique reflexions. (C): $I2/c$, $Z = 4$, $a = 9\cdot15\,(3)$, $b = 24\cdot22\,(8)$, $c = 6\cdot41\,(3)$ Å, $\beta = 93\cdot9\,(1)°$, $U = 1416\,\text{Å}^3$, $D_x = 1\cdot53$ g cm^{-3}, $R = 0\cdot093$, $R_w = 0\cdot077$ for 744 unique reflexions. The crystal structures of the three phases are quite similar. The nearly planar chelate molecules are stacked into columns. The central Ni^{II} ions lie in linear chains parallel to **c**. The monoclinic phase can structurally be formed by a slight parallel shift of the molecule stacks relative to each other along **c**. The components U_{33} of the anisotropic temperature factors are strikingly high for (A) and increase even more on cooling to 160 K, suggesting that the first-order phase transition orthorhombic–monoclinic is driven by the increasing atomic displacements parallel to **c**. In the twinned monoclinic phase a diffuse scattering between strong twin reflexions could be observed. It is explained by a disorder model.

Introduction

The α modification of the investigated compound is of special interest with regard to the existence of an incommensurate modulated phase. Within the scope of the determination of the actual modulated structure and the study of the phase transitions the structures of all

---

* IUPAC name: α-bis(*N*-methylsalicylideneiminato)nickel(II).

phases have been determined or redetermined, respectively.

The structure of A was first refined by Fox & Lingafelter (1967) in the space group $Ibam$ using $hk0$ and $hk1$ reflexions only. A was found to be isostructural with α-CuNSal (Lingafelter, Simmons, Morosin, Scheringer & Freiburg, 1961). Steurer & Adlhart (1981) reported that all phases of α-NiNSal were isotypic with the corresponding α-CuNSal and α-PdNSal modifications. The phase transitions are of the same type but shifted to lower temperatures. The transition temperatures are, for the copper compound, $T_i = 305\,(2)$ and $T_c = 241\,(2)$ K (Adlhart, Blank & Jagodzinski, 1982). The range of stability of the modulated phase is very similar for the two compounds $[\Delta T_{Ni^{II}} = 52\,(5)$ and $\Delta T_{Cu^{II}} = 64$ K$]$.

Experimental

Needle-shaped crystals of α-NiNSal were prepared following the method reported by Adlhart & Syal (1981). The needle axis was parallel to **c**. The intensity data for the room-temperature phase A: Enraf–Nonius CAD-4 four-circle diffractometer, graphite monochromated Mo $K\alpha$ radiation, lattice parameters from least-squares refinement of 25 high-angle reflexions. $\Omega/2\theta$ scans, carried out in the minimal absorption position by rotating around the scattering vector. One standard reflexion, measured every 90 min, I decrease $<3\%$. 2827 reflexions, four octants, $2\theta \leq 70°$, Lorentz and polarization correction, no absorption correction [crystal diameter 0·2 mm, $\mu(\text{Mo } K\alpha) = 12\cdot9$ cm^{-1}]. 1238 averaged reflexions $(R_i = 0\cdot039)$, I (observed) if $I > 0$, weights assigned to the reflexions $w = 1/\sigma^2(F_o)$.

The intensity data for the two low-temperature phases B and C were collected on an automatic Weissenberg diffractometer (AWD) controlled by a PDP-11 computer. A 12 kW Rigaku rotating anode with molybdenum and copper target, respectively, was used as X-ray source. The low-temperature apparatus provided an absolute temperature accuracy of about 2 K and a temperature stability of ±0·2 K (Adlhart & Huber, 1982). Intensity measurements: Ω scans, Mo

$K\alpha$ radiation, focusing quartz monochromator for B, Cu $K\alpha_1$ radiation, focusing germanium monochromator for C. To be independent from changes of the intensity of the primary beam the intensities were measured compared to a constant monitor count rate of 1×10^6. Lattice parameters from nine high-angle reflexions; for the evaluation of the integrated intensities and the separation of TDS and diffuse scattering two Gaussian lines were fitted to the respective reflexion profiles. According to the diffraction geometry corrections for Lorentz and polarization effects were applied in the form

$$1/p = (\tfrac{1}{8} + \tfrac{3}{8}K) + \cos^2 Y \cos^2 v(\tfrac{3}{8} + \tfrac{1}{8}K) + \sin^2 v\tfrac{1}{4}(1 - K).$$

$K = \cos^2 2\theta_m$ for a mosaic crystal, $K = \cos 2\theta_m$ for an ideal crystal, Y, v, see Buerger (1977), $1/l = \sin Y \cos v$. No absorption correction $[\mu(\text{Cu } K\alpha_1) = 17\cdot4 \text{ cm}^{-1}]$. In order to get a complete data set the intensities were measured from all eight octants of the reciprocal sphere; for this purpose the crystal was mounted on the goniometer head parallel to **a** and **c**, respectively. The twin reflexions of C coincide in the layer with $l = 0$ and diverge by an increasing amount for higher layers [twin plane (100)]. Corresponding to the ratio of the intensities of the twin reflexions the intensities of the zero-layer reflexions have been halved $[I(hk0) = I(\bar{h}k0)]$. The overlapping data sets of 2909 (for B) and 1460 (for C) intensities greater than zero were merged and averaged by a least-squares refinement of individual batch scale factors to yield 1480 and 747 independent reflexions (internal consistency factor $R_I = 0\cdot026$ and $0\cdot065$, respectively).

Averaging of the intensity data and refinements of all three structures were performed using SHELX-76 (Sheldrick, 1976) on a Cyber 170 computer. Atomic scattering factors and anomalous-dispersion correction factors were taken from International Tables for X-ray Crystallography (1974).

Structure refinements

The systematic extinctions $hkl:h + k + l = 2n + 1$, $0kl:k = 2n + 1$ and $h0l:h = 2n + 1$ for A and for the main reflexions of B suggest the space groups $Iba2$ or $Ibam$, respectively. In the chosen non-standard setting, which makes allowance for the great structural similarity between the three phases, the monoclinic phase C shows the systematic absences $hkl:h + k + l = 2n + 1$ and $h0l:h = 2n + 1$; therefore the space groups Ic or $I2/c$, subgroups of $Iba2$ and $Ibam$, respectively, are possible. Since the distribution of normalized structure factors is acentric for A only and not unequivocal for B and C, structure refinements were performed in both the centro- and noncentrosymmetric space groups.

The function minimized was $\sum w(|F_o| - |F_c|)^2$, the weighted R factor $R_w = [\sum w(|F_o| - |F_c|)^2/$

$\sum w|F_o|^2]^{1/2}$. A first-order isotropic extinction correction was applied in the refinements. The positional parameters given by Fox & Lingafelter (1967) were used as a starting set. The full-matrix least-squares refinements of the structure A and the average structure B with anisotropic temperature factors for the non-hydrogen atoms in the space group $Iba2$ yielded $R = 0\cdot067$, $R_w = 0\cdot032$ and $R = 0\cdot065$, $R_w = 0\cdot026$, respectively. Hamilton (1965) tests show these values to be significantly better than for refinements in $Ibam$ (A: $R_w^{Ibam}/R_w^{Iba2} = 1\cdot107$, $\mathcal{R}_{35,1109,0\cdot005} = 1\cdot027$; B: $R_w^{Ibam}/R_w^{Iba2} = 1\cdot089$, $\mathcal{R}_{35,1351,0\cdot005} = 1\cdot022$, significance level $\alpha = 0\cdot005$). Because of high correlations between the z parameters and U_{33} it was necessary to introduce a small damping factor to avoid oscillation around the R-factor minimum, when refining the pseudo-centrosymmetric average structure B.

The monoclinic structure C was refined isotropically with the positional parameters of the hydrogen atoms tied to the corresponding carbon atoms. Individual scale factors were refined for the layers with $l = $ constant to allow corrections for different size of the twin individuals and the influence of disorder. As a result the R factors decreased significantly from $R = 0\cdot105$, $R_w = 0\cdot096$ to $R = 0\cdot093$, $R_w = 0\cdot077$. In order to avoid heavy correlations between anisotropic temperature factors and individual layer scale factors isotropic refinement could be performed only. Calculations in the space group Ic did not give significantly better R factors $[R_w^{I2/c}/R_w^{Ic} = 1\cdot025$, $\mathcal{R}_{47,817,0\cdot500} = 1\cdot026$; significance level $\alpha = 0\cdot500$, Hamilton (1965)]. Three very strong reflexions $-$ 110, 002, $\bar{1}12$ $-$ have been omitted because they show severe extinction effects.

Disorder

The introduction of individual layer scale factors ($l = $ constant) led to a significant improvement of the R factors. We will discuss the magnitude of these scale factors with the help of a disorder model.
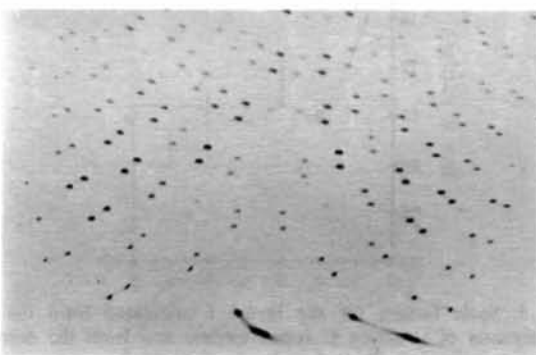

Fig. 1. Section of an $hk2$ normal-beam Weissenberg photograph at $T = 130$ K.

The crystal is twinned in the monoclinic low-temperature structure C, the twin plane is (100) (Fig. 1). The strong twin reflexions are connected by a diffuse streak (Fig. 2) which does not vanish on cooling to 40 K. Therefore, we assume that this diffuse scattering is caused by static disorder. The crystal may be described as made up of a sequence of twin lamellae along **a**, the size of the lamellae being of decisive influence on the intensity of the diffuse scattering and the Bragg reflexions. The model calculations were performed with the domain scattering theory of Adlhart (1981). Following this theory the size of the lamellar domains is described by arbitrary statistical distribution functions, the individual domain sizes being statistically independent from each other. In our special case an asymmetric distribution function of the domain sizes

$$v(\Gamma) = C(1 - 1/\Gamma_0)^\Gamma$$

was chosen. Γ is the individual and Γ_0 the average domain size. The calculation of the intensity profile of a twin reflexion for the layer $l = 2$ and $\Gamma_0 = 40a$ is shown in Fig. 2. The profile was fitted by two Gaussian lines in the same way as in the whole data set for the structure refinements and the intensity of the sharp part was determined. Calculations of profiles for all layers ($l =$ constant) gave the theoretical scale factors. Comparing the experimental and theoretical scale factors (Fig. 3) one can see a qualitatively good agreement except for the layer $l = 0$. The discrepancy for the zero layer may be explained to some extent by slightly unequal twin individuals (the parts by volume of the twin individuals have been determined with a failure of about 5%) and by extinction effects. The extinction effects are smaller for higher layers ($l \neq 0$) because of the broadening of the reflexion profiles due to disorder.
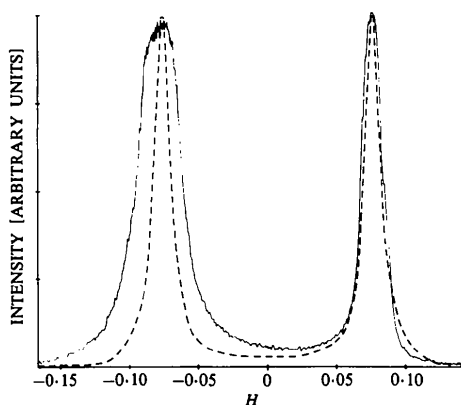
Fig. 2. Photometer curve of the 132 twin reflexion taken from a Weissenberg photograph at 130 K (full line) and the calculated scattering for a twin reflexion of the layer $l = 2$ (broken line).
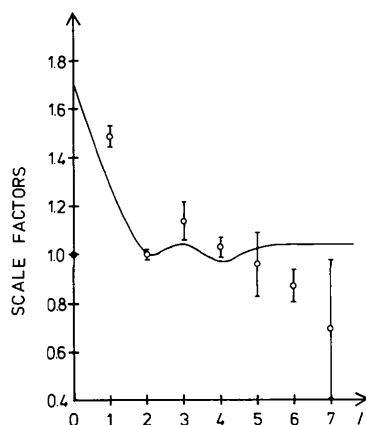
Fig. 3. Scale factors for the layers l calculated from the refinements of structure C (open circles) and from the domain theory (solid line). The values for $l = 2$ were taken as a common scale because the experimental values for $l = 0$ are affected by extinction.

Results and discussion

The final atomic parameters of the three structures are listed in Table 1.* The x and y coordinates do not differ much. The components U_{33} of the anisotropic temperature factors are strikingly high for A and B. While U_{11} and U_{22} are reduced by the expected extent when cooling to 160 K, U_{33} is still growing, e.g. for the Ni^{II} ion from 0·0593 (5) to 0·0875 (5) Å^2 and for the C(8) atom from 0·0581 (87) to 0·1205 (41) Å^2. The z coordinates and U_{13}, U_{23} decrease mostly; this means that the deviations from centrosymmetry become smaller but remain still significant.

The intramolecular distances and angles are given in Fig. 4. The bond Ni^{II}—N is elongated compared with Ni^{II}—O owing to steric interactions between the methyl group and the adjacent O atom. The crystal structure of A projected down **c** is shown in Fig. 5. The molecules are stacked into columns, the Ni^{II} ions lying above one another. The distances Ni^{II}–Ni^{II} are rather long (3·2 to 3·3 Å) compared with the metal bond length of 2·5 Å but there may be a weak interaction between the Ni^{II} ions. The forces between the columns are van der Waals. There is less steric hindrance for shifting the columns adjacent along **a** against each other than for the columns related by centering. The interlocking of these columns over H(C4)—H(C4^i)† becomes more effective upon cooling to 160 K.

In order to get information about the molecular motion and consequently about the mechanism of the phase transition orthorhombic ↔ monoclinic, thermal

---

† The superscript i refers to the adjacent molecule.

Table 1. *Fractional atomic parameters* ($\times 10^4$) *with e.s.d.'s in parentheses*

$U_{eq} = \frac{1}{3}(U_{11} + U_{22} + U_{33})$ for non-hydrogen atoms. The values for A are given in the first line, for B in the second and for C in the third.

	x	y	z	U_{eq}/U ($\text{Å}^2 \times 10^4$)
Ni	0	0	0	470 (4)
	0	0	0	395 (4)
	0	0	0	94 (7)
N	−1210 (4)	635 (2)	9 (19)	520 (28)
	−1201 (3)	639 (1)	14 (20)	408 (16)
	−1225 (8)	650 (3)	−104 (19)	1 (20)
O	1678 (3)	407 (1)	85 (22)	594 (25)
	1696 (2)	409 (1)	−12 (18)	452 (13)
	1714 (6)	410 (2)	205 (17)	1 (16)
C(1)	1873 (6)	943 (2)	47 (25)	503 (31)
	1896 (3)	942 (1)	−87 (21)	378 (20)
	1896 (10)	937 (3)	172 (26)	1 (22)
C(2)	3302 (5)	1148 (2)	229 (30)	585 (47)
	3343 (4)	1149 (1)	65 (28)	501 (21)
	3324 (9)	1145 (3)	285 (25)	1 (23)
H(C2)	4127 (34)	885 (13)	638 (62)	297 (112)
	4133 (26)	831 (9)	630 (38)	22 (61)
	4236 (9)	861 (3)	429 (25)	1 (263)
C(3)	3565 (6)	1698 (2)	−53 (34)	814 (44)
	3613 (4)	1696 (1)	−27 (26)	522 (22)
	3595 (9)	1700 (3)	218 (24)	8 (23)
H(C3)	4551 (36)	1801 (12)	−410 (71)	351 (140)
	4519 (35)	1808 (13)	−378 (62)	515 (73)
	4717 (9)	1841 (3)	267 (24)	361 (362)
C(4)	2442 (7)	2068 (2)	−91 (46)	808 (49)
	2479 (4)	2085 (2)	−29 (24)	537 (21)
	2466 (10)	2090 (3)	89 (25)	25 (24)
H(C4)	2658 (43)	2431 (18)	−424 (67)	373 (125)
	2712 (33)	2506 (10)	−530 (49)	383 (72)
	2691 (10)	2527 (3)	71 (25)	1 (233)
C(5)	1047 (5)	1879 (2)	25 (34)	683 (39)
	1050 (3)	1889 (1)	−12 (22)	434 (20)
	1032 (9)	1886 (3)	−17 (24)	8 (23)
H(C5)	256 (44)	2127 (11)	−496 (77)	330 (131)
	192 (34)	2204 (10)	−349 (58)	348 (70)
	128 (9)	2174 (3)	−151 (24)	338 (311)
C(6)	727 (7)	1318 (2)	−244 (25)	391 (43)
	750 (3)	1328 (1)	−112 (19)	341 (22)
	739 (10)	1322 (3)	47 (25)	1 (25)
C(7)	−753 (6)	1138 (2)	−31 (31)	537 (42)
	−761 (3)	1149 (1)	83 (23)	382 (21)
	−769 (10)	1142 (4)	−93 (25)	22 (25)
H(C7)	−1446 (40)	1406 (16)	−542 (80)	388 (150)
	−1586 (28)	1468 (9)	−414 (45)	184 (61)
	−1593 (10)	1462 (4)	−201 (25)	449 (392)
C(8)	−2829 (5)	582 (2)	−293 (28)	475 (52)
	−2831 (3)	593 (2)	12 (23)	520 (21)
	−2850 (10)	578 (3)	−278 (26)	1 (22)
H(C8)	−3063 (38)	285 (14)	1024 (67)	81 (104)
	−3021 (33)	364 (10)	612 (44)	1 (73)
	−3112 (10)	143 (3)	−271 (26)	1013 (543)
H'(C8)	−3266 (74)	449 (25)	−1915 (130)	1488 (321)
	−3218 (34)	380 (11)	−1550 (44)	50 (63)
	−3298 (10)	762 (3)	−1719 (26)	1172 (701)
H"(C8)	−3262 (32)	926 (12)	576 (58)	45 (100)
	−3339 (39)	975 (13)	−331 (69)	789 (74)
	−3316 (10)	778 (3)	1031 (26)	1149 (695)

Fig. 4. Bond lengths (Å) and angles (°) with e.s.d.'s in parentheses for the phases (*a*) at room temperature (*A*), (*b*) at 160 K (*B*), (*c*) at 40 K (*C*).

motion analyses (**TLS**) (Schomaker & Trueblood, 1968) were calculated with *XANADU* (Roberts & Sheldrick, 1976). The results are tabulated in Table 2. Generally, the calculations show an important increase of the librational and translational motion going from *A* to *B* and the formation of a main libration axis parallel
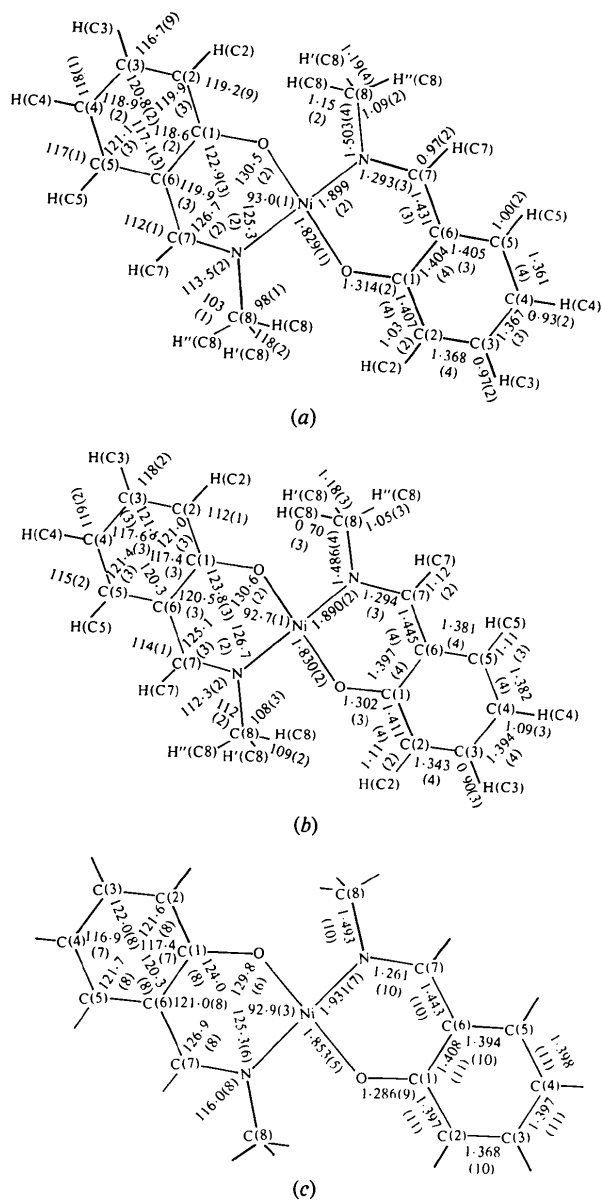
to **b** and a main translation direction parallel to **c**. The *R* factors indicate that the rigid-body model applied to the whole molecule is rather a coarse approximation but the results can be used to illustrate the mechanism of the phase transition. By shifting the columns against each other parallel to **c** the monoclinic structure can be made up. This shift (0·5 Å) and the deviation of the monoclinic angle from 90° (2·8°) at 145 K correspond to the translation term parallel to **c** (0·27 Å) and the libration term around **b** (3·9°) calculated for the 160 K structure. The monoclinic angle increases on cooling (145 K: 92·8°, 40 K: 93·9°). The **TLS**

Table 2. *Thermal motion analysis* (**TLS**) *calculated for the structures A and B assuming the entire and the half-molecule respectively as rigid bodies*

Results for the **T**, **L** and **S** tensors with e.s.d.'s in parentheses are given. R_g gives the agreement between observed and calculated U_{ij}, weights were assigned to the atoms according to their atom number.

(a) Structure A, entire molecule
Center which gives symmetric **S**

0·0000	0·0000	−0·2538

L (rad²)

0·0013 (6)	−0·0003 (5)	0·0000 (4)
	0·0021 (11)	0·0000 (6)
		0·0016 (3)

S (rad Å)

0·0047 (38)	−0·0022 (15)	0·0000 (6)
	−0·0053 (39)	0·0000 (10)
		0·0006 (37)

T (Å²)

0·0401 (80)	0·0171 (50)	0·0000 (42)
	0·0315 (52)	0·0000 (34)
		0·0504 (52)

$R_g = 0·275$

(b) Structure B, entire molecule
Center which gives symmetric **S**

0·0000	0·0000	0·1229

L (rad²)

0·0002 (4)	0·0009 (4)	0·0000 (3)
	0·0046 (8)	0·0000 (4)
		0·0008 (2)

S (rad Å)

−0·0014 (26)	0·0034 (9)	0·0000 (4)
	0·0011 (26)	0·0000 (7)
		0·0003 (25)

T (Å²)

0·0126 (33)	0·0020 (24)	0·0000 (27)
	0·0199 (25)	0·0000 (22)
		0·0756 (35)

$R_g = 0·208$

(c) Structure A, half molecule
Center which gives symmetric **S**

0·0052	0·0571	−0·1189

L (rad²)

0·0034 (34)	−0·0018 (33)	0·0021 (14)
	0·0023 (30)	−0·0002 (13)
		0·0017 (9)

S (rad Å)

0·0058 (48)	−0·0021 (37)	−0·0019 (19)
	−0·0048 (48)	0·0019 (26)
		−0·0010 (39)

T (Å²)

0·0437 (66)	0·0086 (52)	0·0106 (54)
	0·0368 (62)	−0·0110 (48)
		0·0478 (91)

$R_g = 0·238$

(d) Structure B, half molecule
Center which gives symmetric **S**

0·0509	0·0837	0·0580

L (rad²)

0·0048 (18)	0·0014 (18)	0·0010 (8)
	0·0066 (16)	−0·0021 (7)
		0·0008 (5)

S (rad Å)

−0·0013 (23)	0·0006 (16)	−0·0022 (7)
	0·0014 (23)	0·0003 (9)
		−0·0001 (20)

T (Å²)

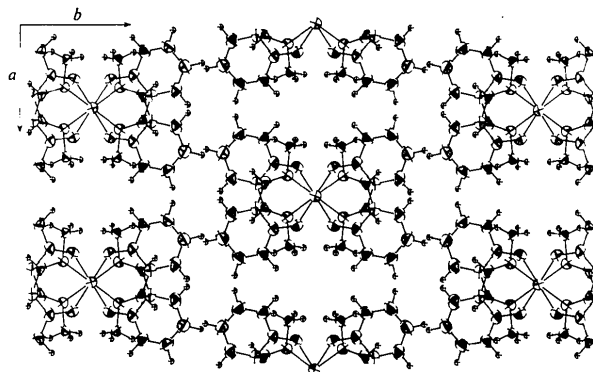|		
0·0124 (27)	0·0001 (22)	0·0018 (29)
	0·0236 (25)	−0·0002 (25)
		0·0605 (50)

$R_g = 0·137$

Fig. 5. Crystal structure of the room-temperature phase of α-NiNSal projected down **c**. The thermal ellipsoids are plotted with a probability level of 50%. The radii of the H atoms are set to 0·1 Å (*ORTEP*, Johnson, 1965).

analysis for the half-molecule gives information about internal motions of the molecules too. The translational tensor remains essentially unaltered but the librational tensor shows a new term parallel to **a**. This can be interpreted as a kind of 'fluttering' motion of the molecule.

The lattice constants, most of all c, decrease on cooling to 160 K though the U_{33} increase strongly in the average structure of B. This can only be explained by the fact that the uncorrelated thermal vibrations of the molecules lying above one another are replaced partially by equally phased displacive modulation waves with amplitudes parallel to **c**. Such a correlated motion of the molecules implies a motion of the entire column. As soon as the shifts of the columns against each other reach a critical magnitude the phase transition occurs. A detailed investigation of the modulated structure, the subject of the following paper (Steurer & Adlhart, 1983), will provide further information.

References

ADLHART, W. (1981). *Acta Cryst.* A37, 794–801.
ADLHART, W., BLANK, H. & JAGODZINSKI, H. (1982). *Acta Cryst.* A38, 505–510.
ADLHART, W. & HUBER, H. (1982). *J. Appl. Cryst.* 15, 241–244.
ADLHART, W. & SYAL, V. K. (1981). *Z. Kristallogr.* 154, 227–233.
BUERGER, M. J. (1977). *Kristallographie*, pp. 150. Berlin, New York: de Gruyter.
FOX, M. R. & LINGAFELTER, E. C. (1967). *Acta Cryst.* 22, 943–944.
HAMILTON, W. C. (1965). *Acta Cryst.* 18, 502–510.
International Tables for X-ray Crystallography (1974). Vol. IV. Birmingham: Kynoch Press.

JOHNSON, C. K. (1965). *ORTEP*. Report ORNL-3794. Oak Ridge National Laboratory, Tennessee.

LINGAFELTER, E. C., SIMMONS, G. L., MOROSIN, B., SCHERINGER, C. & FREIBURG, C. (1961). *Acta Cryst.* **14**, 1222–1225

ROBERTS, P. & SHELDRICK, G. M. (1976). *XANADU*. Univ. of Cambridge, England.

SCHOMAKER, V. & TRUEBLOOD, K. N. (1968). *Acta Cryst.* **B24**, 63–76.

SHELDRICK, G. M. (1976). *SHELX*. A program for crystal structure determination. Univ. of Cambridge, England.

STEURER, W. & ADLHART, W. (1981). *Acta Cryst.* **A37**, C232.

STEURER, W. & ADLHART, W. (1983). *Acta Cryst.* **B39**, 349–355.

The Structure of the Incommensurate Modulated Phase of α-Bis-(N-methylsalicylaldiminato)nickel(II)*

BY W. STEURER AND W. ADLHART

Institut für Kristallographie und Mineralogie der Universität München, Theresienstrasse 41, 8000 München 2, Federal Republic of Germany

Abstract

The modulated structure of the title compound (α-NiNSal) was determined at 160 K by single-crystal X-ray methods. The refinements were performed in the superspace group $P^{Iba2}_{11\bar{1}}$ (α00). Different models considering thermal fluctuations in the phase and the amplitude of the static modulation wave were calculated. The best refinement yielded the overall R factors $R = 0.088$, $R_w = 0.051$ for 4322 independent reflexions including 2725 first-order and 118 second-order reflexions. The positional parameters of the basic structure and of the average structure are nearly equal. The amplitudes of the one-dimensional displacive modulation waves decrease due to steric interactions between adjacent molecule stacks from 0·30 Å at the central Ni^{II} ion to 0·22 Å at the peripheral C atoms. The modulation functions were found to be sinusoidal. Calculations with a phason factor yielded only slightly better R factors – no reliable proof for the existence of amplitude and phase fluctuations.

Introduction

Incommensurate modulated structures undergo a periodical displacement of the atoms from the positions of the basic structure and/or are modulated in the occupation probabilities or magnetic moments of the atoms. The period of this modulation is incommensurate relative to the period of the basic structure. Until now only a few modulated structures were determined and most of the investigations were dealing with both displacive and occupation probability modulation, for example Toman & Frueh (1976a,b), Kitamura & Morimoto (1977), Böhm (1978), Horst, Tagai, Korekawa & Jagodzinski (1981), Yamamoto & Nakazawa (1982) and Yamamoto (1982). Very few refinements were carried out on mere displacively modulated structures as for example on γ-Na_2CO_3 (van Aalst, den Hollander, Peterse & de Wolff, 1976). But just these structures and the phase transitions commensurate – incommensurate mostly associated with them are of special interest owing to new lattice dynamical properites (see Axe, 1976, for a review). It is expected that, in addition to the normal modes, there exist phasons and amplitudons corresponding to fluctuations of phase and amplitude of the modulation wave (Overhauser, 1971; Axe, 1980). More recent investigations on biphenyl (Cailleau, Moussa, Zeyen & Bouillot, 1980) show the existence of a phason branch. Theoretical studies of Moncton, Axe & di Salvo (1977) revealed that the ground state of an incommensurate structure does not consist of a mere sinusoidal distortion. Anharmonic interactions always cause additional distortions, being higher harmonics of the primary modulation. The difficulty of proving the existence of smaller anharmonic contributions without a refinement of the modulated structure is because the diffraction harmonics of the primary modulation and the scattering contributions of the higher harmonics coincide. Additional complications result from the influence of the phase and amplitude fluctuations of the static distortion wave.

The intention of the present work was to provide further information about the influence of phasons, amplitudons and higher harmonics besides the determination of the individual modulation functions.

---

* IUPAC name: α-bis(N-methylsalicylideneiminato)nickel(II).